

Research Paper

# Analysis of a Functionally Graded Finite Wedge Under Antiplane Deformation

A.R. Shahani<sup>1,\*</sup>, I. Shakeri<sup>2</sup>

<sup>1</sup>Faculty of Mechanical Engineering, Department of Applied Mechanics, K.N. Toosi University of Technology, Tehran, Iran

<sup>2</sup>Laboratory of Fracture Mechanics, Department of Applied Mechanics, K.N. Toosi University of Technology, Tehran, Iran

Received 22 March 2022; accepted 25 May 2022

## ABSTRACT

The antiplane deformation of a wedge made of a functionally graded material (FGM) with finite radius has been investigated analytically in the present article. In relation to the boundary conditions imposed on the arc portion of the wedge, displacement or traction, two problems have been studied. In each of the problems three various kinds of boundary conditions (traction-displacement, displacement-displacement and traction-traction) have been applied to the radial edges of the wedge. The governing differential equations have been solved by employing finite Fourier transforms and Green's function method. The closed form solutions for stress and displacement distribution have been achieved for the whole domain. Explicit relations have been extracted for the order of stress singularity in all cases. These relations indicated the dependence of the order of stress singularity on the boundary conditions, material property and wedge angle. In fact, despite of an isotropic wedge, for which the order of stress singularity depends only the geometry of the wedge, in an FG wedge the order of stress singularity depends both the geometry as well as the material property.

© 2022 IAU, Arak Branch. All rights reserved.

**Keywords :** Antiplane shear deformation; FGM wedge; Stress singularity; Finite Fourier transforms; Green's function method.

## 1 INTRODUCTION

**W**EDGE is one of the popular and familiar geometries and due to its different applications the researches have been encouraged to deal with the analysis of wedges. A wedge is capable to be modeled in different angles from  $0^\circ$  to  $360^\circ$  and it can produce other important problems and geometries. Lap joints, shafts and edge-cracked are some examples for wedge-like geometries applications. The wedge stress analysis with infinite radius was conducted by some researchers using the classical linear theory of elasticity. The plane elasticity problem of an

\*Corresponding author. Tel.: +98 21 84063221; Fax.: +98 21 88677273.  
E-mail address: shahani@kntu.ac.ir (A.R. Shahani)

isotropic infinite wedge was solved by Tranter [1] using the Airy stress function and Mellin transform. Then, Williams [2] by employing the eigen-function expansion method investigated the stress singularity at the wedge apex. The plane elasticity problem of anisotropic infinite wedges was studied by Bogy [3] and Kuo and Bogy [4,5] using generalized Mellin transform. Dempsey and Sinclair [6] studied the singularity of stress at the apex of a composite wedge subjected to in-plane loading. Assuming that the stresses near the apex are of the order  $O(r^{-\lambda})$ , they found the order of stress singularity,  $\lambda$ , at the wedge apex from the solution of a characteristic equation of the form  $|K(\lambda) = 0|$ . Also, they strove to predict a logarithmic singularity of the form  $O(r^{-\lambda} \log r)$  at the wedge apex from the solution of the related characteristic equation. The main weakness of their approach is that it can not specify the wedge angles in which the logarithmic singularity happens. In a series of papers, Dempsey [7] and Ting [8,9] discussed the paradox which existed in the elementary solution of an elastic wedge. Ting [9] considered an expansion form of the harmonic eigen functions and then, by applying suitable boundary conditions, obtained the coefficients of this expansion. The problem of antiplane deformation of dissimilar anisotropic wedge with infinite radius was formulated by Ma and Hour [10], however it was only able to derive the equation of poles and extract the strength of singularity in special cases. Later on, Kargarnovin et al. [11] obtained stress distribution of the isotropic finite wedges under antiplane shear deformation for various boundary conditions using finite Mellin transformations of the first and second kinds. The strength of the singularities were derived from the resulting analytic relations for the stress fields. Problems involving infinite isotropic wedges were then analyzed by letting the radius of the finite wedges tend to infinity. Shahani [12] solved the problem of antiplane shear loading of anisotropic finite wedges by defining some complex integral transformations. The circular boundary of the wedge was subjected to the traction-free condition, and three kinds of boundary conditions were applied on the radial edges, i.e., traction-traction, displacement-displacement, and displacement-traction. Afterward, Shahani and Adibnazari [13] studied the antiplane shear deformation of perfectly bonded wedges as well as bonded wedges with an interface crack. The solution of governing differential equations is accomplished by means of the Mellin transform. For two edge-bonded isotropic wedges with perfect bonding along the common edge, closed form solutions were obtained for stress fields and analytical relations were given for the order of stress singularity at the apex. Shahani [14] analyzed the antiplane deformation of several wedges with an interface crack. He considered three types of materials for wedges: isotropic, anisotropic and bonded dissimilar materials. The stress intensity factors were analytically extracted for some practical cases such as rounded shafts with edge cracks, bonded wedges having an interfacial edge crack, bonded half planes including an interfacial edge crack and double cantilever beams with different boundary conditions. Faal et al. [15] investigated an isotropic infinite wedge impaired by a screw dislocation. They studied numerically the effect of wedge angle and the location and orientation of the crack on the stress intensity factors of straight line cracks. Using the Mellin transform with the aid of image method, displacement and stress fields of the dissimilar isotropic annular wedges under antiplane loading was obtained by Lin and Ma [16]. Shahani [17] analyzed a bi-material finite wedge subjected to antiplane shear deformation with different boundary conditions. The solution of governing differential equations is accomplished by means of finite Mellin transforms. The closed form solutions are obtained for displacement and stress fields in the entire domain. The geometric singularities of stress fields are observed to be dependent on material property, in general. However, in the special case of equal apex angles in the traction traction problem, this dependency ceases to exist and the geometric singularity shows dependency only upon the apex angle. Later, Shahani [18] extracted mode III stress intensity factor for a crack located at the interface of dissimilar bonded wedges. In the case when the sum of the two apex angles is equal to  $2\pi$ , the problem reduces to that of two edge-bonded dissimilar materials with an interfacial crack subjected to concentrated antiplane shear tractions on the crack faces. By using the image method, Faal et al. [19] studied an isotropic wedge with a finite radius under different boundary conditions damaged by multiple cavities. The integral equations are of the Cauchy singular kind and are solved numerically to determine hoop stress on the cavities. The closed form solutions for the stress and displacement distribution in the isotropic finite wedge under antiplane deformation were obtained by Shahani [20]. The main advantages of these closed form solutions is to explicitly show both the possible geometric and load singularities, in addition to the continuity or discontinuity as well as the convergence of the results in the entire region. Furthermore, as a practical case, the stress intensity factors for an edge crack in a circular shaft subjected to several boundary conditions were derived. Chen et al. [21] studied the composite wedge with a finite radius subjected to antiplane deformation. Antiplane shear loading was applied to the circular segment and three types of displacement boundary conditions were considered for the radial edges (free-free, fixed-fixed and free-fixed). By defining new finite complex transforms, Shahani and Ghadiri [22] solved the problem of two edge-bonded isotropic finite wedges with an interfacial crack subjected to antiplane deformation. Traction boundary conditions were considered for both radial edges. They introduced new finite complex transforms to solve the

governing partial differential equations. Also, Shahani and Ghadiri [23] considered an anisotropic sector with a radial crack, and obtained the stress intensity factors at both ends of the crack numerically. Ghadiri and Shahani [24] studied the problem of non-isotropic cracked wedges with finite length, and plotted the stress intensity factors at both ends of the crack under various conditions. Later on, Ghadiri and Shahani [25] solved the problem of bonded anisotropic finite wedges with a radial crack under antiplane deformation by introducing new finite complex transforms. Traction-free was prescribed on the circular part of the wedge, and the radial edges were under displacement-displacement boundary conditions. The order of stress singularities which was explicitly derived indicated its dependence on the boundary conditions, material constants and wedge angle. Eder and Sarhadi [26] proposed a method to correct the numerical near singularity stress field in vicinity of reentrant corners by a semi-analytical solution. Their approach pertains to perfectly bonded bi-material interface V-notches with arbitrary opening angles under Mode-III loading. Their method addresses dissimilar joints with sharp corners in large-scale numerical engineering models where high-resolution discretization becomes computationally expensive. Their method is therefore particularly useful for fatigue lifetime analysis of shear-bending dominated large utility multi material structures such as compound castings, aircraft wings and wind turbine rotor blades to name a few. The solution for the governing Laplace equation is obtained by separation of variables in conjunction with the eigenvalue expansion method yielding the bi-material notch singularity exponent.

The aim of the present study is to analytically analyze an FGM wedge with finite radius subjected to antiplane deformation. Depending upon the type of boundary data applied to the circular part of the wedge, two problems are considered. In problems I and II, the arc fragment of the wedge is subjected to the traction free and fixed displacement conditions, respectively. Three different types of boundary conditions were prescribed on the radial edges of the wedge for each problem: traction-displacement, displacement-displacement and traction-traction. The tractions are presumed to apply concentrically that permits the solutions to be used as the Green's function in order to analyze a wedge subjected to arbitrary distribution of traction. The solution is achieved by using the finite Fourier transforms and the Green's function method. The closed form solutions for the stress and displacement distribution are attained for the whole domain. Despite of an isotropic wedge, for which the order of stress singularity depends only the geometry of the wedge, in an FG wedge the order of stress singularity depend both the geometry as well as the material property. Eventually, it is indicated, as expected, that in the particular case of a wedge with infinite radius, both problems produce the same results. In the particular case of a wedge with isotropic materials, the results of the reduced problem are perfectly identical to that published by Kargamovin et al. [11].

## 2 FORMULATION AND PROBLEM SOLUTION

Consider an FGM wedge with apex angle  $\alpha$ , radius  $a$  and non-finite length in the vertical direction to the wedge plane (Fig. 1).

The antiplane shear deformation is applied on the wedge as a condition. It indicates that the out of plane component of displacement,  $w$ , is the only non-vanishing component and it is stated as a function of coordinates  $r$  and  $\theta$ . Consequently,  $\tau_{rz}(r, \theta)$  and  $\tau_{\theta z}(r, \theta)$  are the non-zero stress components. Thereafter, the constitutive equations for Functionally Graded Material reduce to:

$$\begin{aligned}\tau_{rz} &= 2\mu\epsilon_{rz} = \mu \frac{\partial w}{\partial r} \\ \tau_{\theta z} &= 2\mu\epsilon_{\theta z} = \frac{\mu}{r} \frac{\partial w}{\partial \theta}\end{aligned}\quad (1)$$

where  $\mu$  denotes the shear modulus of the material which is variable along the wedge and it is assumed its variations is according to the Eq. (2):

$$\mu(r) = \mu_0 r^m, \quad m > 0 \quad (2)$$

In which  $\mu_0$  and  $m$  are material constants. The equilibrium equations in cylindrical coordinate may be expressed as:

$$\begin{aligned} \frac{\partial \sigma_r}{\partial r} + \frac{\sigma_r - \sigma_\theta}{r} + \frac{1}{r} \frac{\partial \tau_{r\theta}}{\partial \theta} + \frac{\partial \tau_{rz}}{\partial z} + F_r &= 0 \\ \frac{\partial \tau_{r\theta}}{\partial r} + \frac{2\tau_{r\theta}}{r} + \frac{1}{r} \frac{\partial \sigma_\theta}{\partial \theta} + \frac{\partial \tau_{\theta z}}{\partial z} + F_\theta &= 0 \\ \frac{\partial \tau_{rz}}{\partial r} + \frac{\tau_{rz}}{r} + \frac{1}{r} \frac{\partial \tau_{\theta z}}{\partial \theta} + \frac{\partial \sigma_z}{\partial z} + F_z &= 0 \end{aligned} \tag{3}$$

By using Eqs. (1) and (2) and the assumption of non-appearance of body forces, the third equation of equilibrium appears in terms of displacement according to the Eq. (4):

$$r^2 \frac{\partial^2 w}{\partial r^2} + r(1+m) \frac{\partial w}{\partial r} + \frac{\partial^2 w}{\partial \theta^2} = 0 \tag{4}$$

In problem I, i.e., cases Ia, Ib and Ic, traction-free boundary condition is prescribed on the circular segment of the wedge (Fig. 1(a, b, c)). Hence

$$\tau_{rz}(a, \theta) = 0 \tag{5}$$

In problem II, i.e., cases IIa, IIb and IIc, arc part of the wedge boundary is fixed (Fig. 1(d, e, f)). Therefore

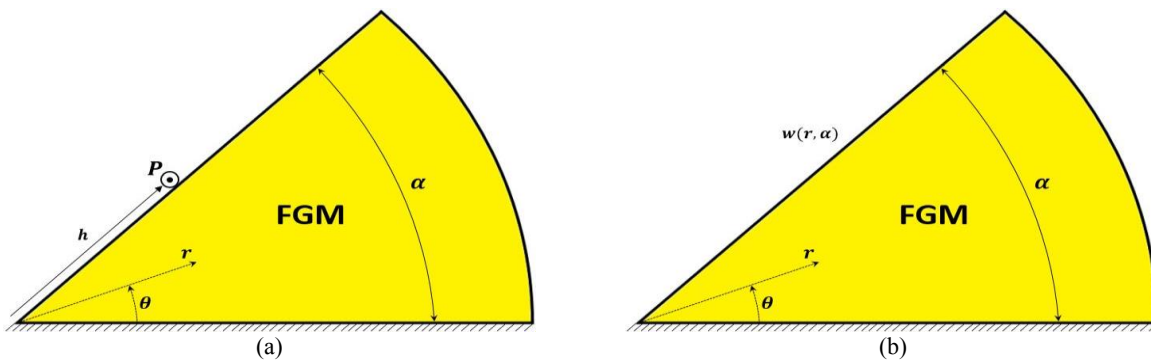
$$w(a, \theta) = 0 \tag{6}$$

For a finite wedge the solution of Eq. (3) may be achieved by employing the finite Fourier transform and Green's function method, respectively. The finite Fourier transform is defined as [27]:

$$F[w(r, \theta), n] = W^*(r, n) = \int_0^\alpha k(n, \theta) w(r, \theta) d\theta \tag{7}$$

where  $k(n, \theta)$  is the kernel of transform and it is defined according to the boundary conditions prescribed on the radial edges of the wedge, as it is obtained from the solution of Eq. (3) with homogeneous boundary conditions. The inversion of this transform is represented as:

$$F^{-1}[W^*(r, n), \theta] = w(r, \theta) = \sum_{n=0}^\infty \frac{k(n, \theta)}{\int_0^\alpha k^2(n, \theta) d\theta} W^*(r, n) \tag{8}$$



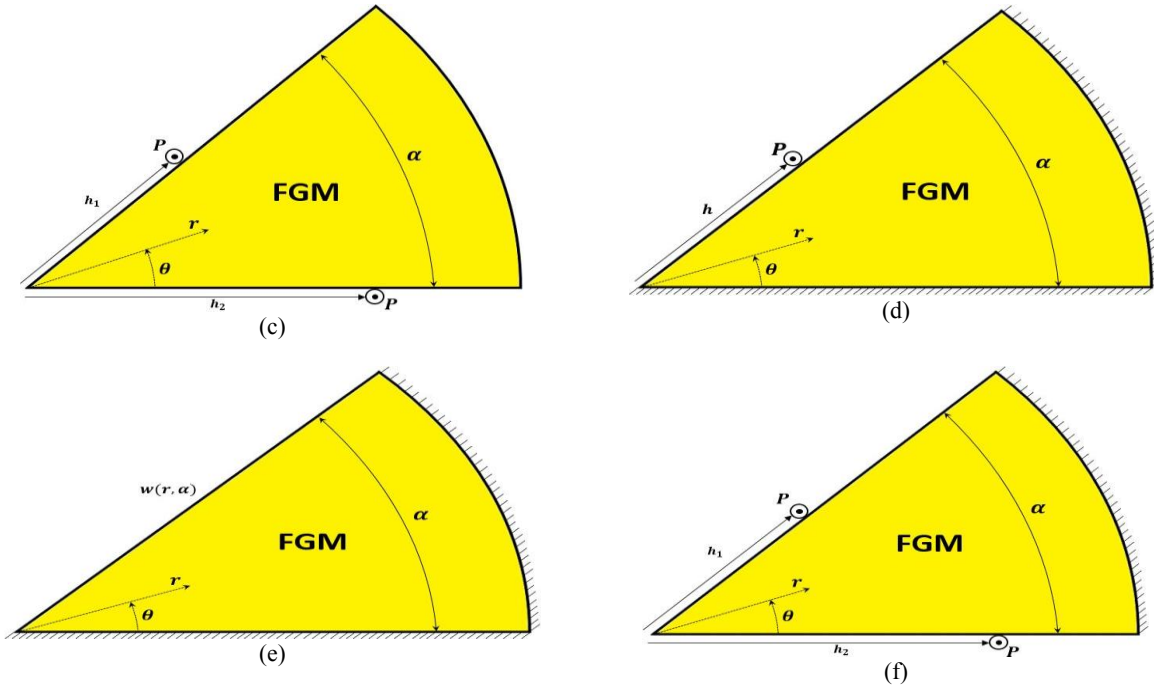


**Fig.1**  
Schematic view of the applied boundary conditions to the finite wedge for the problems (a) Ia (b) Ib (c) Ic (d) IIa (e) IIb (f) IIc.

### 3 PROBLEM I

In each problem, based on the imposed conditions on the radial edges of the wedge, three various cases may be considered as: traction-displacement, displacement-displacement and traction-traction. In this section, these cases are studied for Problem I one by one.

#### 3.1 Case Ia: Traction-Displacement

In this case, one radial edge of the wedge is fixed and the other one is under antiplane shear traction. Thus, the following boundary conditions may be expressed

$$\begin{aligned}
 w(r, 0) &= 0 \\
 \tau_{\theta z}(r, \alpha) &= P\delta(r - h) \quad 0 < h < a
 \end{aligned} \tag{9}$$

where  $\delta$  designates the Dirac-Delta function. It is noteworthy to indicate that the choice of the second conditions of (9), results in the Green's function solution for the problem. For the boundary data (9) the corresponding finite Fourier transform has the following form

$$W_{ss}^*(r, n) = \int_0^\alpha w(r, \theta) \sin\left[\frac{(2n+1)\pi}{2\alpha}\theta\right] d\theta \tag{10}$$

Applying the Fourier transform (10) in conjunction with integration by parts on (4), leads to

$$r^2 \frac{d^2 W_{ss}^*}{dr^2} + r(1+m) \frac{dW_{ss}^*}{dr} - \frac{(2n+1)^2 \pi^2}{4\alpha^2} W_{ss}^* + (-1)^n \frac{\partial w(r, \alpha)}{\partial \theta} + \frac{(2n+1)\pi}{2\alpha} w(r, 0) = 0 \tag{11}$$

Applying the boundary data (9) on (11) leads to the following equation

$$r^2 \frac{d^2 W_{ss}^*}{dr^2} + r(1+m) \frac{dW_{ss}^*}{dr} - \beta_n^2 W_{ss}^* = \varphi_n r^{1-m} \delta(r-h) = f_a(r) \tag{12}$$

where

$$\beta_n^2 = \frac{(2n+1)^2 \pi^2}{4\alpha^2} \quad \varphi_n = -\frac{P}{\mu_0} (-1)^n \tag{13}$$

The Green’s function method [28,29] may be used to derive a general solution to an inhomogeneous boundary value problem (12). To determine the Green’s function, the following boundary value problem should be solved:

$$r^2 \frac{d^2 G(r, \xi)}{dr^2} + r(1+m) \frac{dG(r, \xi)}{dr} - \beta_n^2 G(r, \xi) = \delta(r - \xi) \tag{14}$$

with

$$G(0, \xi) = 0 \quad \partial G(a, \xi) / \partial r = 0 \tag{15}$$

In order to find the Green’s function, the problem should be split up on two domains,  $r \in [0, \xi]$  and  $r \in (\xi, a]$ . In each domain the homogeneous equation with homogeneous boundary condition should be solved separately. On those domains, since  $r \neq \xi$

$$r^2 \frac{d^2 G(r, \xi)}{dr^2} + r(1+m) \frac{dG(r, \xi)}{dr} - \beta_n^2 G(r, \xi) = 0 \tag{16}$$

The general solution of Eq. (16) is as follows:

$$G(r, \xi) = C_1(\xi)r^{u_1} + C_2(\xi)r^{u_2} \tag{17}$$

where  $C_1$  and  $C_2$  are arbitrary functions of  $\xi$  and

$$u_1 = \frac{-m + \sqrt{m^2 + 4\beta_n^2}}{2} \quad u_2 = \frac{-m - \sqrt{m^2 + 4\beta_n^2}}{2} \tag{18}$$

It should be noted that always  $u_1 > 0$  and  $u_2 < 0$ . In the left hand interval  $[0, \xi]$  it requires the Green’s function to satisfy the homogeneous governing equation (except at  $r = \xi$ ) and the left hand boundary condition. Similarly, in the right hand interval,  $(\xi, a]$ , the Green’s function satisfies the homogeneous governing equation and the right hand boundary condition. Denoting the left hand solution as:

$$G_1(r, \xi) = C_1(\xi)r^{u_1} + C_2(\xi)r^{u_2} \tag{19}$$

with  $G_1(0, \xi) = 0$  this gives  $C_2(\xi) = 0$ . Therefore

$$G_1(r, \xi) = C_1(\xi)r^{u_1} \tag{20}$$

Similarly in the right domain, with

$$G_2(r, \xi) = C_3(\xi)r^{u_1} + C_4(\xi)r^{u_2} \quad (21)$$

It is found that  $\partial G(a, \xi)/\partial r = 0$  gives

$$C_4(\xi) = -C_3(\xi) \frac{u_1}{u_2} a^{u_1-u_2} \quad (22)$$

Substituting (22) in (21), yields

$$G_2(r, \xi) = C_3(\xi) \left( r^{u_1} - \frac{u_1}{u_2} a^{u_1-u_2} r^{u_2} \right) \quad (23)$$

Hence, the Green's function can be written as:

$$G(r, \xi) = \begin{cases} C_1(\xi)r^{u_1} & 0 \leq r < \xi \\ C_3(\xi) \left( r^{u_1} - \frac{u_1}{u_2} a^{u_1-u_2} r^{u_2} \right) & \xi < r \leq a \end{cases} \quad (24)$$

Two conditions are required to determine the constants.  $G(r, \xi)$  must be continuous at  $r = \xi$ , which means that

$$C_1 \xi^{u_1} - C_3 \left( \xi^{u_1} - \frac{u_1}{u_2} a^{u_1-u_2} \xi^{u_2} \right) = 0 \quad (25)$$

A second condition can be found by integrating the governing Eq. (14) from  $\xi - \epsilon$  to  $\xi + \epsilon$  and then letting  $\epsilon \rightarrow 0$ . This yields

$$\left. \frac{dG(r, \xi)}{dr} \right|_{r=\xi^+} - \left. \frac{dG(r, \xi)}{dr} \right|_{r=\xi^-} = \frac{1}{\xi^2} \quad (26)$$

which means that the derivative of the Green's function is discontinuous across the unit impulse. By substituting (24) in (26), the second condition appears as:

$$C_3 \left( u_1 \xi^{u_1-1} - u_1 a^{u_1-u_2} \xi^{u_2-1} \right) - C_1 u_1 \xi^{u_1-1} = \frac{1}{\xi^2} \quad (27)$$

Solving the Eqs. (25) and (27),  $C_1(\xi)$  and  $C_3'(\xi)$  are obtained and the Green's functions of the problem is determined as:

$$G(r, \xi) = \begin{cases} \frac{\left( \frac{u_2}{u_1} a^{u_2-u_1} \xi^{-1-u_2} - \xi^{-1-u_1} \right) r^{u_1}}{u_1 - u_2} & 0 \leq r \leq \xi \\ \frac{\left( \frac{u_2}{u_1} a^{u_2-u_1} r^{u_1} - r^{u_2} \right) \xi^{-1-u_2}}{u_1 - u_2} & \xi \leq r \leq a \end{cases} \quad (28)$$

The Heaviside (unit) step function is defined by

$$H(t) = \begin{cases} 1 & t > 0 \\ 0 & t < 0 \end{cases} \tag{29}$$

So the Green’s function may be expressed as:

$$G(r, \xi) = \frac{\left(\frac{u_2}{u_1} a^{u_2-u_1} \xi^{-1-u_2} - \xi^{-1-u_1}\right) r^{u_1}}{u_1-u_2} H(\xi-r) + \frac{\left(\frac{u_2}{u_1} a^{u_2-u_1} r^{u_1} - r^{u_2}\right) \xi^{-1-u_2}}{u_1-u_2} H(r-\xi) \tag{30}$$

The general solution of the ODE (12) is

$$\begin{aligned} W_{ss}^* &= \int_0^a G(r, \xi) f_a(\xi) d\xi \\ &= \int_0^a \left[ \frac{\left(\frac{u_2}{u_1} a^{u_2-u_1} \xi^{-1-u_2} - \xi^{-1-u_1}\right) r^{u_1}}{u_1-u_2} H(\xi-r) + \frac{\left(\frac{u_2}{u_1} a^{u_2-u_1} r^{u_1} - r^{u_2}\right) \xi^{-1-u_2}}{u_1-u_2} H(r-\xi) \right] f_a(\xi) d\xi \\ &= \int_0^r \frac{\left(\frac{u_2}{u_1} a^{u_2-u_1} r^{u_1} - r^{u_2}\right) \xi^{-1-u_2}}{u_1-u_2} \varphi_n \xi^{1-m} \delta(\xi-h) d\xi + \int_r^a \frac{\left(\frac{u_2}{u_1} a^{u_2-u_1} \xi^{-1-u_2} - \xi^{-1-u_1}\right) r^{u_1}}{u_1-u_2} \varphi_n \xi^{1-m} \delta(\xi-h) d\xi \end{aligned} \tag{31}$$

In the region  $0 \leq r < h$  the first integral and in the region  $h < r \leq a$  the second integral of (31) are vanished. The transformed displacement, then, appears as:

$$W_{ss}^*(r, n) = \begin{cases} \frac{\varphi_n h^{-m}}{u_1-u_2} \left[ \frac{u_2}{u_1} \left(\frac{a}{h}\right)^{u_2} \left(\frac{r}{a}\right)^{u_1} - \left(\frac{r}{h}\right)^{u_1} \right] & 0 \leq r \leq h \\ \frac{\varphi_n h^{-m}}{u_1-u_2} \left[ \frac{u_2}{u_1} \left(\frac{a}{h}\right)^{u_2} \left(\frac{r}{a}\right)^{u_1} - \left(\frac{r}{h}\right)^{u_2} \right] & h \leq r \leq a \end{cases} \tag{32}$$

Making use of Eqs. (8) and (13), the inversion of (32) results in

$$w(r, \theta) = \begin{cases} \frac{2P}{\alpha \mu_0 h^m} \sum_{n=0}^{\infty} \frac{(-1)^n}{u_1-u_2} \left[ \left(\frac{r}{h}\right)^{u_1} - \frac{u_2}{u_1} \left(\frac{a}{h}\right)^{u_2} \left(\frac{r}{a}\right)^{u_1} \right] \sin \left[ \frac{(2n+1)\pi}{2\alpha} \theta \right] & r \leq h \\ \frac{2P}{\alpha \mu_0 h^m} \sum_{n=0}^{\infty} \frac{(-1)^n}{u_1-u_2} \left[ \left(\frac{r}{h}\right)^{u_2} - \frac{u_2}{u_1} \left(\frac{a}{h}\right)^{u_2} \left(\frac{r}{a}\right)^{u_1} \right] \sin \left[ \frac{(2n+1)\pi}{2\alpha} \theta \right] & h \leq r \end{cases} \tag{33}$$

Substituting (33) in (1), stress components are obtained as:

$$\tau_{rz}(r, \theta) = \begin{cases} \frac{2P}{\alpha h^m} \sum_{n=0}^{\infty} \frac{(-1)^n}{u_1-u_2} r^{m-1} \left[ u_1 \left(\frac{r}{h}\right)^{u_1} - u_2 \left(\frac{a}{h}\right)^{u_2} \left(\frac{r}{a}\right)^{u_1} \right] \sin \left[ \frac{(2n+1)\pi}{2\alpha} \theta \right] & r < h \\ \frac{2P}{\alpha h^m} \sum_{n=0}^{\infty} \frac{(-1)^n u_2}{u_1-u_2} r^{m-1} \left[ \left(\frac{r}{h}\right)^{u_2} - \left(\frac{a}{h}\right)^{u_2} \left(\frac{r}{a}\right)^{u_1} \right] \sin \left[ \frac{(2n+1)\pi}{2\alpha} \theta \right] & h < r \end{cases} \tag{34}$$

$$\tau_{\theta z}(r, \theta) = \begin{cases} \frac{P\pi}{\alpha^2 h^m} \sum_{n=0}^{\infty} \frac{(-1)^n (2n+1)}{u_1 - u_2} r^{m-1} \left[ \left(\frac{r}{h}\right)^{u_1} - \frac{u_2}{u_1} \left(\frac{a}{h}\right)^{u_2} \left(\frac{r}{a}\right)^{u_1} \right] \cos \left[ \frac{(2n+1)\pi}{2\alpha} \theta \right] & r \leq h \\ \frac{P\pi}{\alpha^2 h^m} \sum_{n=0}^{\infty} \frac{(-1)^n (2n+1)}{u_1 - u_2} r^{m-1} \left[ \left(\frac{r}{h}\right)^{u_2} - \frac{u_2}{u_1} \left(\frac{a}{h}\right)^{u_2} \left(\frac{r}{a}\right)^{u_1} \right] \cos \left[ \frac{(2n+1)\pi}{2\alpha} \theta \right] & h \leq r \end{cases} \quad (35)$$

Eqs. (33) to (35) indicate that at the act point of traction, the series solutions for displacement and stress component  $\tau_{rz}$  are divergent. Furthermore, on the arc  $r = h$ , the value of  $\tau_{rz}$  is discontinuous. It is perceived from the first of Eqs. (34) and (35) that the stress components are bounded in a wedge apex with  $0 < \alpha < \frac{\pi}{2\sqrt{1-m}}$ , while in a wedge with  $\frac{\pi}{2\sqrt{1-m}} < \alpha < 2\pi$ , stress components have the following form

$$(\tau_{rz}, \tau_{\theta z}) = O(r^{-\lambda}) \quad \text{as } r \rightarrow 0 \quad (36)$$

and the strength of geometric singularity is

$$\lambda = 1 - (u_1 + m) = 1 - \frac{m}{2} \left[ 1 + \sqrt{1 + \left(\frac{\pi}{m\alpha}\right)^2} \right] \quad (37)$$

It can be seen that in an FG wedge the order of stress singularity depends both the geometry as well as the material property. Fig. 2 shows the variation of strength of geometric singularity versus material property for various wedge angles. As can be seen from Fig. 2, the strength of singularity decreases by decreasing the apex angle and for the wedge with apex angle  $\alpha \leq \pi/2$ , no geometric singularity is observed. Also, the strength of singularity decreases by increasing  $m$  and for the FG wedge with material property  $m \geq 1$  the geometric singularity vanishes. It should be noted that in the particular case of an isotropic wedge, i.e.  $m = 0$ , the strength of geometric singularity will be  $\lambda = 1 - \pi/(2\alpha)$  and the results of the reduced problem are perfectly identical to that published by Kargarnovin et al. [11]. By applying  $a \rightarrow \infty$  in (33) to (35), the stress and displacement fields can be attained for the particular case of a wedge with infinite radius. Merely the displacement component is stated for brevity's sake:

$$w(r, \theta) = \begin{cases} \frac{2P}{\alpha\mu_0 h^m} \sum_{n=0}^{\infty} \frac{(-1)^n}{u_1 - u_2} \left(\frac{r}{h}\right)^{u_1} \sin \left[ \frac{(2n+1)\pi}{2\alpha} \theta \right] & 0 \leq r \leq h \\ \frac{2P}{\alpha\mu_0 h^m} \sum_{n=0}^{\infty} \frac{(-1)^n}{u_1 - u_2} \left(\frac{r}{h}\right)^{u_2} \sin \left[ \frac{(2n+1)\pi}{2\alpha} \theta \right] & h \leq r \leq a \end{cases} \quad (38)$$

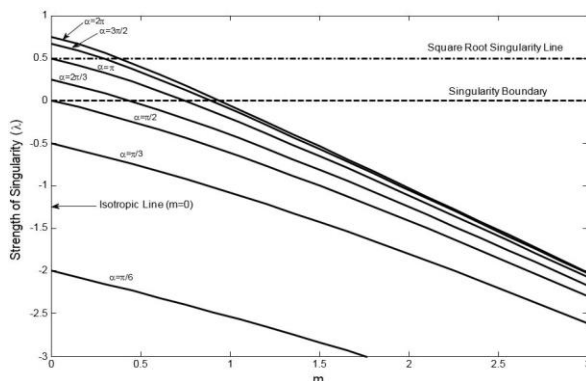


**Fig.2** The variation of strength of geometric singularity versus material property for various wedge angles.

3.2 Case Ib: Displacement-Displacement

In this case, the wedge is considered to be fixed on the edge  $\theta = 0$  and under antiplane deformation on the boundary  $\theta = \alpha$ . Therefore, the boundary conditions for Eq. (4) may be expressed as the following form

$$w(r, 0) = 0 \quad w(r, \alpha) = r^k, \quad k > 0 \tag{39}$$

where  $k$  is a real constant. It is worth mentioning that any displacement boundary conditions on the edge  $\theta = \alpha$  may be generally represented by its Taylor series expansion at  $r = 0$ . The second condition of (39) is the general form of a term of such series. For the boundary conditions (39) the finite Fourier transform has the following form

$$W_s^*(r, n) = \int_0^\alpha w(r, \theta) \sin\left(\frac{n\pi}{\alpha} \theta\right) d\theta \tag{40}$$

Applying the Fourier transform (40) in conjunction with integration by parts on (4) results in

$$r^2 \frac{d^2 W_s^*}{dr^2} + r(1+m) \frac{dW_s^*}{dr} - \frac{n^2 \pi^2}{\alpha^2} W_s^* + \frac{n\pi}{\alpha} \{w(r, 0) - (-1)^n w(r, \alpha)\} = 0 \tag{41}$$

The application of boundary conditions (39) on (41) leads to the following equation

$$r^2 \frac{d^2 W_s^*}{dr^2} + r(1+m) \frac{dW_s^*}{dr} - \beta_n^2 W_s^* = \varphi_n r^k = f_b(r) \tag{42}$$

where

$$\beta_n^2 = \frac{n^2 \pi^2}{\alpha^2} \quad \varphi_n = \frac{n\pi}{\alpha} (-1)^n \tag{43}$$

The general forms of the homogeneous Eqs. (42) and (12) are the same. Therefore, the Green's function of Eq. (42) is the same as (30). The general solution of the ODE (42) is as follows:

$$\begin{aligned} W_s^*(r, n) &= \int_0^a G(r, \xi) f_b(\xi) d\xi \\ &= \int_0^a \left[ \frac{\left(\frac{u_2}{u_1} a^{u_2-u_1} \xi^{-1-u_2} - \xi^{-1-u_1}\right) r^{u_1}}{u_1-u_2} H(r-\xi) + \frac{\left(\frac{u_2}{u_1} a^{u_2-u_1} r^{u_1} - r^{u_2}\right) \xi^{-1-u_2}}{u_1-u_2} H(\xi-r) \right] \varphi_n \xi^k d\xi \\ &= \int_0^r \frac{\left(\frac{u_2}{u_1} a^{u_2-u_1} r^{u_1} - r^{u_2}\right) \xi^{-1-u_2}}{u_1-u_2} \varphi_n \xi^k d\xi + \int_r^a \frac{\left(\frac{u_2}{u_1} a^{u_2-u_1} \xi^{-1-u_2} - \xi^{-1-u_1}\right) r^{u_1}}{u_1-u_2} \varphi_n \xi^k d\xi \end{aligned} \tag{44}$$

For  $u_1 \neq k$  which appears in a wedge with angle  $\alpha \neq \frac{n'\pi}{\sqrt{k^2 + mk}}$  where  $n'$  is a positive integer, the transformed displacement by calculation of integrals of (44) and with the aid of (18) reduces to

$$W_s^*(r, n) = \frac{\varphi_n}{k^2 + mk - \beta_n^2} r^k \left[ 1 - \frac{k}{u_1} \left( \frac{r}{a} \right)^{u_1 - k} \right] \quad (45)$$

Using the inversion formula (8), the displacement is determined as:

$$w(r, \theta) = \frac{2\pi}{\alpha^2} \sum_{n=1}^{\infty} \frac{n(-1)^n}{k^2 + mk - \beta_n^2} r^k \left[ 1 - \frac{k}{u_1} \left( \frac{r}{a} \right)^{u_1 - k} \right] \sin\left(\frac{n\pi}{\alpha} \theta\right) \quad (46)$$

Substituting (46) in (1), stress fields are obtained as:

$$\begin{aligned} \tau_{rz}(r, \theta) &= \frac{2\pi\mu_0 k}{\alpha^2} \sum_{n=1}^{\infty} \frac{n(-1)^n}{k^2 + mk - \beta_n^2} r^{m+k-1} \left[ 1 - \left( \frac{r}{a} \right)^{u_1 - k} \right] \sin\left(\frac{n\pi}{\alpha} \theta\right) \\ \tau_{\theta z}(r, \theta) &= \frac{2\pi^2 \mu_0}{\alpha^3} \sum_{n=1}^{\infty} \frac{n^2 (-1)^n}{k^2 + mk - \beta_n^2} r^{m+k-1} \left[ 1 - \frac{k}{u_1} \left( \frac{r}{a} \right)^{u_1 - k} \right] \cos\left(\frac{n\pi}{\alpha} \theta\right) \end{aligned} \quad (47)$$

As can be seen from stress solutions (47), the first terms of the series parts are singular at the wedge apex, where  $\alpha > \frac{\pi}{\sqrt{1-m}}$  and the order of stress singularity may be determined from the following expression

$$\lambda = 1 - (u_1 + m) = 1 - \frac{m}{2} \left[ 1 + \sqrt{1 + \left( \frac{2\pi}{m\alpha} \right)^2} \right] \quad (48)$$

Similar to the previous case, when  $m = 0$ , we arrive at the solution for an isotropic wedge which coincides with the results of that published by Kargarnovin et al. [11].

### 3.3 Case Ic: Traction-Traction

In this case, both the radial edges of the wedge are considered under antiplane shear tractions. The boundary conditions are expressed as:

$$\begin{aligned} \tau_{\theta z}(r, 0) &= P\delta(r - h_2) \\ \tau_{\theta z}(r, \alpha) &= P\delta(r - h_1) \end{aligned} \quad (49)$$

Without loss of generality, it is presumed that  $h_1 \leq h_2$ . For the boundary data (49) the finite Fourier transform has the following form

$$W_c^*(r, n) = \int_0^\alpha w(r, \theta) \cos\left(\frac{n\pi}{\alpha} \theta\right) d\theta \quad (50)$$

The application of Fourier transform (50) in conjunction with integration by parts on (4) leads to

$$r^2 \frac{d^2 W_c^*}{dr^2} + r(1+m) \frac{dW_c^*}{dr} - \frac{n^2 \pi^2}{\alpha^2} W_c^* - \frac{\partial w(r, 0)}{\partial \theta} + (-1)^n \frac{\partial w(r, \alpha)}{\partial \theta} = 0 \quad (51)$$

Applying the boundary conditions (49) on (51) results in the following equation

$$r^2 \frac{d^2 W_c}{dr^2} + r(1+m) \frac{dW_c}{dr} - \beta_n^2 W_c = \varphi r^{1-m} \left[ (-1)^n \delta(r-h_1) - \delta(r-h_2) \right] = f_c(r) \tag{52}$$

where

$$\beta_n^2 = \frac{n^2 \pi^2}{\alpha^2} \quad \varphi = -\frac{P}{\mu_0} \tag{53}$$

The general forms of the homogeneous Eqs. (52) and (12) are identical. Thus, the Green’s function of Eq. (52) is the same as (30). The general solution of the ODE (52) is obtained as follows:

$$\begin{aligned} W_c^* = & \int_0^a G(r, \xi) f_c(\xi) d\xi = \int_0^r \frac{\left( \frac{u_2}{u_1} a^{u_2-u_1} r^{u_1} - r^{u_2} \right) \xi^{-1-u_2}}{u_1 - u_2} \varphi \xi^{1-m} (-1)^n \delta(\xi - h_1) d\xi \\ & - \int_0^r \frac{\left( \frac{u_2}{u_1} a^{u_2-u_1} r^{u_1} - r^{u_2} \right) \xi^{-1-u_2}}{u_1 - u_2} \varphi \xi^{1-m} \delta(\xi - h_2) d\xi + \int_r^a \frac{\left( \frac{u_2}{u_1} a^{u_2-u_1} \xi^{-1-u_2} - \xi^{-1-u_1} \right) r^{u_1}}{u_1 - u_2} \varphi \xi^{1-m} (-1)^n \delta(\xi - h_1) d\xi \\ & - \int_r^a \frac{\left( \frac{u_2}{u_1} a^{u_2-u_1} \xi^{-1-u_2} - \xi^{-1-u_1} \right) r^{u_1}}{u_1 - u_2} \varphi \xi^{1-m} \delta(\xi - h_2) d\xi \end{aligned} \tag{54}$$

In the region  $0 \leq r < h_1$  the first and second integral, in the region  $h_1 < r < h_2$  the second and third integral and in the region  $h_2 < r \leq a$  the third and fourth integral of (54) are vanished. Thus, the transformed displacement appears as:

$$\begin{aligned} W_c^*(r, n) = & \frac{\varphi}{u_1 - u_2} \left\{ (-1)^n h_1^{-m} \left[ \frac{u_2}{u_1} \left( \frac{a}{h_1} \right)^{u_2} \left( \frac{r}{a} \right)^{u_1} - \left( \frac{r}{h_1} \right)^{u_1} \right] \right. \\ & \left. - h_2^{-m} \left[ \frac{u_2}{u_1} \left( \frac{a}{h_2} \right)^{u_2} \left( \frac{r}{a} \right)^{u_1} - \left( \frac{r}{h_2} \right)^{u_1} \right] \right\} \quad 0 \leq r \leq h_1 \end{aligned} \tag{55a}$$

$$\begin{aligned} W_c^*(r, n) = & \frac{\varphi}{u_1 - u_2} \left\{ (-1)^n h_1^{-m} \left[ \frac{u_2}{u_1} \left( \frac{a}{h_1} \right)^{u_2} \left( \frac{r}{a} \right)^{u_1} - \left( \frac{r}{h_1} \right)^{u_2} \right] \right. \\ & \left. - h_2^{-m} \left[ \frac{u_2}{u_1} \left( \frac{a}{h_2} \right)^{u_2} \left( \frac{r}{a} \right)^{u_1} - \left( \frac{r}{h_2} \right)^{u_1} \right] \right\} \quad h_1 \leq r \leq h_2 \end{aligned} \tag{55b}$$

$$\begin{aligned} W_c^*(r, n) = & \frac{\varphi}{u_1 - u_2} \left\{ (-1)^n h_1^{-m} \left[ \frac{u_2}{u_1} \left( \frac{a}{h_1} \right)^{u_2} \left( \frac{r}{a} \right)^{u_1} - \left( \frac{r}{h_1} \right)^{u_2} \right] \right. \\ & \left. - h_2^{-m} \left[ \frac{u_2}{u_1} \left( \frac{a}{h_2} \right)^{u_2} \left( \frac{r}{a} \right)^{u_1} - \left( \frac{r}{h_2} \right)^{u_2} \right] \right\} \quad h_2 \leq r \leq a \end{aligned} \tag{55c}$$

Making use of (8), the result of inverse transform yields

$$w(r, \theta) = \frac{2P}{\alpha\mu_0} \sum_{n=1}^{\infty} \frac{1}{u_1 - u_2} \left\{ (-1)^n h_1^{-m} \left[ \left( \frac{r}{h_1} \right)^{u_1} - \frac{u_2}{u_1} \left( \frac{a}{h_1} \right)^{u_2} \left( \frac{r}{a} \right)^{u_1} \right] \right. \\ \left. - h_2^{-m} \left[ \left( \frac{r}{h_2} \right)^{u_1} - \frac{u_2}{u_1} \left( \frac{a}{h_2} \right)^{u_2} \left( \frac{r}{a} \right)^{u_1} \right] \right\} \cos\left(\frac{n\pi}{\alpha} \theta\right) \quad 0 \leq r \leq h_1 \quad (56a)$$

$$w(r, \theta) = \frac{2P}{\alpha\mu_0} \sum_{n=1}^{\infty} \frac{1}{u_1 - u_2} \left\{ (-1)^n h_1^{-m} \left[ \left( \frac{r}{h_1} \right)^{u_2} - \frac{u_2}{u_1} \left( \frac{a}{h_1} \right)^{u_2} \left( \frac{r}{a} \right)^{u_1} \right] \right. \\ \left. - h_2^{-m} \left[ \left( \frac{r}{h_2} \right)^{u_1} - \frac{u_2}{u_1} \left( \frac{a}{h_2} \right)^{u_2} \left( \frac{r}{a} \right)^{u_1} \right] \right\} \cos\left(\frac{n\pi}{\alpha} \theta\right) \quad h_1 \leq r \leq h_2 \quad (56b)$$

$$w(r, \theta) = \frac{2P}{\alpha\mu_0} \sum_{n=1}^{\infty} \frac{1}{u_1 - u_2} \left\{ (-1)^n h_1^{-m} \left[ \left( \frac{r}{h_1} \right)^{u_2} - \frac{u_2}{u_1} \left( \frac{a}{h_1} \right)^{u_2} \left( \frac{r}{a} \right)^{u_1} \right] \right. \\ \left. - h_2^{-m} \left[ \left( \frac{r}{h_2} \right)^{u_2} - \frac{u_2}{u_1} \left( \frac{a}{h_2} \right)^{u_2} \left( \frac{r}{a} \right)^{u_1} \right] \right\} \cos\left(\frac{n\pi}{\alpha} \theta\right) \quad h_2 \leq r \leq a \quad (56c)$$

The stress fields are obtained by substituting (56) into the constitutive Eqs. (1)

$$\tau_{rz}(r, \theta) = \frac{2P}{\alpha} \sum_{n=1}^{\infty} \frac{r^{m-1}}{u_1 - u_2} \left\{ (-1)^n h_1^{-m} \left[ u_1 \left( \frac{r}{h_1} \right)^{u_1} - u_2 \left( \frac{a}{h_1} \right)^{u_2} \left( \frac{r}{a} \right)^{u_1} \right] \right. \\ \left. - h_2^{-m} \left[ u_1 \left( \frac{r}{h_2} \right)^{u_1} - u_2 \left( \frac{a}{h_2} \right)^{u_2} \left( \frac{r}{a} \right)^{u_1} \right] \right\} \cos\left(\frac{n\pi}{\alpha} \theta\right) \quad 0 \leq r < h_1 \quad (57a)$$

$$\tau_{rz}(r, \theta) = \frac{2P}{\alpha} \sum_{n=1}^{\infty} \frac{r^{m-1}}{u_1 - u_2} \left\{ (-1)^n u_2 h_1^{-m} \left[ \left( \frac{r}{h_1} \right)^{u_2} - \left( \frac{a}{h_1} \right)^{u_2} \left( \frac{r}{a} \right)^{u_1} \right] \right. \\ \left. - h_2^{-m} \left[ u_1 \left( \frac{r}{h_2} \right)^{u_1} - u_2 \left( \frac{a}{h_2} \right)^{u_2} \left( \frac{r}{a} \right)^{u_1} \right] \right\} \cos\left(\frac{n\pi}{\alpha} \theta\right) \quad h_1 < r < h_2 \quad (57b)$$

$$\tau_{rz}(r, \theta) = \frac{2P}{\alpha} \sum_{n=1}^{\infty} \frac{u_2 r^{m-1}}{u_1 - u_2} \left\{ (-1)^n h_1^{-m} \left[ \left( \frac{r}{h_1} \right)^{u_2} - \left( \frac{a}{h_1} \right)^{u_2} \left( \frac{r}{a} \right)^{u_1} \right] \right. \\ \left. - h_2^{-m} \left[ \left( \frac{r}{h_2} \right)^{u_2} - \left( \frac{a}{h_2} \right)^{u_2} \left( \frac{r}{a} \right)^{u_1} \right] \right\} \cos\left(\frac{n\pi}{\alpha} \theta\right) \quad h_2 < r \leq a \quad (57c)$$

$$\tau_{\theta z}(r, \theta) = \frac{2\pi P}{\alpha^2} \sum_{n=1}^{\infty} \frac{nr^{m-1}}{u_1 - u_2} \left\{ (-1)^n h_1^{-m} \left[ \frac{u_2}{u_1} \left( \frac{a}{h_1} \right)^{u_2} \left( \frac{r}{a} \right)^{u_1} - \left( \frac{r}{h_1} \right)^{u_1} \right] - h_2^{-m} \left[ \frac{u_2}{u_1} \left( \frac{a}{h_2} \right)^{u_2} \left( \frac{r}{a} \right)^{u_1} - \left( \frac{r}{h_2} \right)^{u_1} \right] \right\} \sin\left(\frac{n\pi}{\alpha} \theta\right) \quad 0 \leq r < h_1 \tag{58a}$$

$$\tau_{\theta z}(r, \theta) = \frac{2\pi P}{\alpha^2} \sum_{n=1}^{\infty} \frac{nr^{m-1}}{u_1 - u_2} \left\{ (-1)^n h_1^{-m} \left[ \frac{u_2}{u_1} \left( \frac{a}{h_1} \right)^{u_2} \left( \frac{r}{a} \right)^{u_1} - \left( \frac{r}{h_1} \right)^{u_2} \right] - h_2^{-m} \left[ \frac{u_2}{u_1} \left( \frac{a}{h_2} \right)^{u_2} \left( \frac{r}{a} \right)^{u_1} - \left( \frac{r}{h_2} \right)^{u_1} \right] \right\} \sin\left(\frac{n\pi}{\alpha} \theta\right) \quad h_1 < r < h_2 \tag{58b}$$

$$\tau_{\theta z}(r, \theta) = \frac{2\pi P}{\alpha^2} \sum_{n=1}^{\infty} \frac{nr^{m-1}}{u_1 - u_2} \left\{ (-1)^n h_1^{-m} \left[ \frac{u_2}{u_1} \left( \frac{a}{h_1} \right)^{u_2} \left( \frac{r}{a} \right)^{u_1} - \left( \frac{r}{h_1} \right)^{u_2} \right] - h_2^{-m} \left[ \frac{u_2}{u_1} \left( \frac{a}{h_2} \right)^{u_2} \left( \frac{r}{a} \right)^{u_1} - \left( \frac{r}{h_2} \right)^{u_2} \right] \right\} \sin\left(\frac{n\pi}{\alpha} \theta\right) \quad h_2 < r \leq a \tag{58c}$$

The line  $\theta = \alpha/2$  is the symmetry line for the particular case of  $h_1 = h_2$ . As a result,  $w(r, \alpha/2) = 0$ , and it can be seen that the solutions (56) to (58) are the same as those of a wedge subjected to traction-displacement boundary condition, case Ia, with apex angle half of the wedge propounded here.

Similar to the traction-displacement case, at the act point of traction, the series solutions for stress and displacement component,  $\tau_{rz}$ , are divergent. In addition, on the arcs  $r = h_1$  and  $r = h_2$ , the value of  $\tau_{rz}$  is discontinuous. It can be seen from the first of Eqs. (57) and (58) that the stress components  $\tau_{rz}$  and  $\tau_{\theta z}$  are bonded in a wedge with apex angle  $0 < \alpha < \frac{\pi}{\sqrt{1-m}}$ . While in a wedge with angle  $\frac{\pi}{\sqrt{1-m}} < \alpha < 2\pi$ , the strength of geometric singularity is

$$\lambda = 1 - \frac{m}{2} \left[ 1 + \sqrt{1 + \left( \frac{2\pi}{m\alpha} \right)^2} \right] \tag{59}$$

which is the same as the geometric singularity of the displacement-displacement case. It should be mentioned that in the special case of an isotropic wedge ( $m = 0$ ), we reach the same results as published by Kargarnovin et al. [11].

By letting  $a \rightarrow \infty$  in (56) to (58), the displacement and stress fields can be achieved for a wedge with infinite radius. Merely the displacement component is expressed here.

$$w(r, \theta) = \begin{cases} \frac{2P}{\alpha\mu_0} \sum_{n=1}^{\infty} \frac{1}{u_1 - u_2} \left[ (-1)^n h_1^{-m} \left( \frac{r}{h_1} \right)^{u_1} - h_2^{-m} \left( \frac{r}{h_2} \right)^{u_1} \right] \cos\left(\frac{n\pi}{\alpha} \theta\right) & 0 \leq r \leq h_1 \\ \frac{2P}{\alpha\mu_0} \sum_{n=1}^{\infty} \frac{1}{u_1 - u_2} \left[ (-1)^n h_1^{-m} \left( \frac{r}{h_1} \right)^{u_2} - h_2^{-m} \left( \frac{r}{h_2} \right)^{u_1} \right] \cos\left(\frac{n\pi}{\alpha} \theta\right) & h_1 \leq r \leq h_2 \\ \frac{2P}{\alpha\mu_0} \sum_{n=1}^{\infty} \frac{1}{u_1 - u_2} \left[ (-1)^n h_1^{-m} \left( \frac{r}{h_1} \right)^{u_2} - h_2^{-m} \left( \frac{r}{h_2} \right)^{u_2} \right] \cos\left(\frac{n\pi}{\alpha} \theta\right) & h_2 \leq r \leq a \end{cases} \tag{60}$$

#### 4 PROBLEM II

The analysis of problem II is fundamentally similar to problem I. Thus, the analysis has been summarized in this problem. As previous, three aforementioned cases of boundary conditions are considered for the radial edges of the wedge.

##### 4.1 Case IIa: Traction-Displacement

Taking a similar line of approach, the Green's function of (14) with following boundary conditions may be obtained

$$G(0, \xi) = 0 \quad G(a, \xi) = 0 \quad (61)$$

By doing similar calculation and with the aid of the boundary conditions (61), finally, the Green's functions of this problem is determined as:

$$G(r, \xi) = \frac{(a^{u_2-u_1} \xi^{-1-u_2} - \xi^{-1-u_1}) r^{u_1}}{u_1 - u_2} H(\xi - r) + \frac{(a^{u_2-u_1} r^{u_1} - r^{u_2}) \xi^{-1-u_2}}{u_1 - u_2} H(r - \xi) \quad (62)$$

The general solution of the ODE (12) is

$$W_{ss}^* = \int_0^a G(r, \xi) f_a(\xi) d\xi = \int_0^r \frac{(a^{u_2-u_1} r^{u_1} - r^{u_2}) \xi^{-1-u_2}}{u_1 - u_2} \varphi_n \xi^{1-m} \delta(\xi - h) d\xi + \int_r^a \frac{(a^{u_2-u_1} \xi^{-1-u_2} - \xi^{-1-u_1}) r^{u_1}}{u_1 - u_2} \varphi_n \xi^{1-m} \delta(\xi - h) d\xi \quad (63)$$

The transformed displacement, then, appears as:

$$W_{ss}^*(r, n) = \begin{cases} \frac{\varphi_n h^{-m}}{u_1 - u_2} \left[ \left(\frac{a}{h}\right)^{u_2} \left(\frac{r}{a}\right)^{u_1} - \left(\frac{r}{h}\right)^{u_1} \right] & 0 \leq r \leq h \\ \frac{\varphi_n h^{-m}}{u_1 - u_2} \left[ \left(\frac{a}{h}\right)^{u_2} \left(\frac{r}{a}\right)^{u_1} - \left(\frac{r}{h}\right)^{u_2} \right] & h \leq r \leq a \end{cases} \quad (64)$$

Using the inversion formula (8), the displacement is determined

$$w(r, \theta) = \begin{cases} \frac{2P}{\alpha \mu_0 h^m} \sum_{n=0}^{\infty} \frac{(-1)^n}{u_1 - u_2} \left[ \left(\frac{r}{h}\right)^{u_1} - \left(\frac{a}{h}\right)^{u_2} \left(\frac{r}{a}\right)^{u_1} \right] \sin \left[ \frac{(2n+1)\pi}{2\alpha} \theta \right] & 0 \leq r \leq h \\ \frac{2P}{\alpha \mu_0 h^m} \sum_{n=0}^{\infty} \frac{(-1)^n}{u_1 - u_2} \left[ \left(\frac{r}{h}\right)^{u_2} - \left(\frac{a}{h}\right)^{u_2} \left(\frac{r}{a}\right)^{u_1} \right] \sin \left[ \frac{(2n+1)\pi}{2\alpha} \theta \right] & h \leq r \leq a \end{cases} \quad (65)$$

Substituting (65) in (1), stress components are attained as:

$$\tau_{rz}(r, \theta) = \begin{cases} \frac{2P}{\alpha h^m} \sum_{n=0}^{\infty} \frac{(-1)^n u_1}{u_1 - u_2} r^{m-1} \left[ \left(\frac{r}{h}\right)^{u_1} - \left(\frac{a}{h}\right)^{u_2} \left(\frac{r}{a}\right)^{u_1} \right] \sin \left[ \frac{(2n+1)\pi}{2\alpha} \theta \right] & 0 \leq r < h \\ \frac{2P}{\alpha h^m} \sum_{n=0}^{\infty} \frac{(-1)^n}{u_1 - u_2} r^{m-1} \left[ u_2 \left(\frac{r}{h}\right)^{u_2} - u_1 \left(\frac{a}{h}\right)^{u_2} \left(\frac{r}{a}\right)^{u_1} \right] \sin \left[ \frac{(2n+1)\pi}{2\alpha} \theta \right] & h < r \leq a \end{cases} \quad (66)$$

$$\tau_{\theta z}(r, \theta) = \begin{cases} \frac{P\pi}{\alpha^2 h^m} \sum_{n=0}^{\infty} \frac{(-1)^n (2n+1)}{u_1 - u_2} r^{m-1} \left[ \left(\frac{r}{h}\right)^{u_1} - \left(\frac{a}{h}\right)^{u_2} \left(\frac{r}{a}\right)^{u_1} \right] \cos \left[ \frac{(2n+1)\pi}{2\alpha} \theta \right] & 0 \leq r \leq h \\ \frac{P\pi}{\alpha^2 h^m} \sum_{n=0}^{\infty} \frac{(-1)^n (2n+1)}{u_1 - u_2} r^{m-1} \left[ \left(\frac{r}{h}\right)^{u_2} - \left(\frac{a}{h}\right)^{u_2} \left(\frac{r}{a}\right)^{u_1} \right] \cos \left[ \frac{(2n+1)\pi}{2\alpha} \theta \right] & h \leq r \leq a \end{cases} \quad (67)$$

The solution for an isotropic wedge is achieved by placing  $m = 0$  in (65) to (67), and the results are completely identical to that published by Kargarnovin et al. [11].

It is apparent that in a wedge with infinite radius, this case should convert to case Ia, owing to the fact that at infinity the displacement and stress components tend to zero. The verification of the statement may easily be obtained by letting  $a \rightarrow \infty$  in (65) and reproducing (38).

#### 4.2 Case IIb: Displacement-Displacement

Analogous to case Ib, the Green's functions of Eq. (42) with the boundary data (61) is the same as (62). The general solution of the ODE (42) is

$$\begin{aligned} W_s^*(r, n) &= \int_0^a G(r, \xi) f_b(\xi) d\xi \\ &= \int_0^r \frac{(a^{u_2 - u_1} r^{u_1} - r^{u_2}) \xi^{-1 - u_2}}{u_1 - u_2} \varphi_n \xi^k d\xi + \int_r^a \frac{(a^{u_2 - u_1} \xi^{-1 - u_2} - \xi^{-1 - u_1}) r^{u_1}}{u_1 - u_2} \varphi_n \xi^k d\xi \end{aligned} \quad (68)$$

For  $u_1 \neq k$  which appears in a wedge with angle  $\alpha \neq \frac{n'\pi}{\sqrt{k^2 + mk}}$ , the transformed displacement with the aid of (18) reduces to

$$W_s^*(r, n) = \frac{\varphi_n}{k^2 + mk - \beta_n^2} r^k \left[ 1 - \left(\frac{r}{a}\right)^{u_1 - k} \right] \quad (69)$$

The application of inversion formula, (8), on this equation gives

$$w(r, \theta) = \frac{2\pi}{\alpha^2} \sum_{n=1}^{\infty} \frac{n(-1)^n}{k^2 + mk - \beta_n^2} r^k \left[ 1 - \left(\frac{r}{a}\right)^{u_1 - k} \right] \sin\left(\frac{n\pi}{\alpha} \theta\right) \quad (70)$$

Components of stress are determined by substituting (56) in the constitutive relationships (1)

$$\begin{aligned} \tau_{rz}(r, \theta) &= \frac{2\pi\mu_0}{\alpha^2} \sum_{n=1}^{\infty} \frac{n(-1)^n}{k^2 + mk - \beta_n^2} r^{m+k-1} \left[ k - u_1 \left(\frac{r}{a}\right)^{u_1 - k} \right] \sin\left(\frac{n\pi}{\alpha} \theta\right) \\ \tau_{\theta z}(r, \theta) &= \frac{2\pi^2\mu_0}{\alpha^3} \sum_{n=1}^{\infty} \frac{n^2(-1)^n}{k^2 + mk - \beta_n^2} r^{m+k-1} \left[ 1 - \left(\frac{r}{a}\right)^{u_1 - k} \right] \cos\left(\frac{n\pi}{\alpha} \theta\right) \end{aligned} \quad (71)$$

As in the previous cases when  $m = 0$ , the results of the problem are in agreement with that published by Kargarnovin et al. [11].

## 4.3 Case IIc: Traction-Traction

Similar to case Ic, the Green's functions of Eq. (52) is the same as (62). The general solution of the ODE (52) is

$$\begin{aligned}
 W_c^* &= \int_0^a G(r, \xi) f_c(\xi) d\xi = \int_0^r \frac{(a^{u_2-u_1} r^{u_1} - r^{u_2}) \xi^{-1-u_2}}{u_1-u_2} \varphi \xi^{1-m} (-1)^n \delta(\xi-h_1) d\xi \\
 &- \int_0^r \frac{(a^{u_2-u_1} r^{u_1} - r^{u_2}) \xi^{-1-u_2}}{u_1-u_2} \varphi \xi^{1-m} \delta(\xi-h_2) d\xi + \int_r^a \frac{(a^{u_2-u_1} \xi^{-1-u_2} - \xi^{-1-u_1}) r^{u_1}}{u_1-u_2} \varphi \xi^{1-m} (-1)^n \delta(\xi-h_1) d\xi \\
 &- \int_r^a \frac{(a^{u_2-u_1} \xi^{-1-u_2} - \xi^{-1-u_1}) r^{u_1}}{u_1-u_2} \varphi \xi^{1-m} \delta(\xi-h_2) d\xi
 \end{aligned} \quad (72)$$

The transformed displacement, then, appears as:

$$W_c^*(r, n) = \begin{cases} \frac{\varphi}{u_1-u_2} \left\{ (-1)^n h_1^{-m} \left[ \left( \frac{a}{h_1} \right)^{u_2} \left( \frac{r}{a} \right)^{u_1} - \left( \frac{r}{h_1} \right)^{u_1} \right] - h_2^{-m} \left[ \left( \frac{a}{h_2} \right)^{u_2} \left( \frac{r}{a} \right)^{u_1} - \left( \frac{r}{h_2} \right)^{u_1} \right] \right\} & 0 \leq r \leq h_1 \\ \frac{\varphi}{u_1-u_2} \left\{ (-1)^n h_1^{-m} \left[ \left( \frac{a}{h_1} \right)^{u_2} \left( \frac{r}{a} \right)^{u_1} - \left( \frac{r}{h_1} \right)^{u_2} \right] - h_2^{-m} \left[ \left( \frac{a}{h_2} \right)^{u_2} \left( \frac{r}{a} \right)^{u_1} - \left( \frac{r}{h_2} \right)^{u_1} \right] \right\} & h_1 \leq r \leq h_2 \\ \frac{\varphi}{u_1-u_2} \left\{ (-1)^n h_1^{-m} \left[ \left( \frac{a}{h_1} \right)^{u_2} \left( \frac{r}{a} \right)^{u_1} - \left( \frac{r}{h_1} \right)^{u_2} \right] - h_2^{-m} \left[ \left( \frac{a}{h_2} \right)^{u_2} \left( \frac{r}{a} \right)^{u_1} - \left( \frac{r}{h_2} \right)^{u_2} \right] \right\} & h_2 \leq r \leq a \end{cases} \quad (73)$$

Making use of the invers transform, (8), the displacement field appears as:

$$\begin{aligned}
 w(r, \theta) &= \frac{2P}{\alpha \mu_0} \sum_{n=1}^{\infty} \frac{1}{u_1-u_2} \left\{ (-1)^n h_1^{-m} \left[ \left( \frac{r}{h_1} \right)^{u_1} - \left( \frac{a}{h_1} \right)^{u_2} \left( \frac{r}{a} \right)^{u_1} \right] \right. \\
 &\left. - h_2^{-m} \left[ \left( \frac{r}{h_2} \right)^{u_1} - \left( \frac{a}{h_2} \right)^{u_2} \left( \frac{r}{a} \right)^{u_1} \right] \right\} \cos\left(\frac{n\pi}{\alpha} \theta\right) \quad 0 \leq r \leq h_1
 \end{aligned} \quad (74a)$$

$$\begin{aligned}
 w(r, \theta) &= \frac{2P}{\alpha \mu_0} \sum_{n=1}^{\infty} \frac{1}{u_1-u_2} \left\{ (-1)^n h_1^{-m} \left[ \left( \frac{r}{h_1} \right)^{u_2} - \left( \frac{a}{h_1} \right)^{u_2} \left( \frac{r}{a} \right)^{u_1} \right] \right. \\
 &\left. - h_2^{-m} \left[ \left( \frac{r}{h_2} \right)^{u_1} - \left( \frac{a}{h_2} \right)^{u_2} \left( \frac{r}{a} \right)^{u_1} \right] \right\} \cos\left(\frac{n\pi}{\alpha} \theta\right) \quad h_1 \leq r \leq h_2
 \end{aligned} \quad (74b)$$

Substitution of (74) in (1) results in the stress components

$$\begin{aligned}
 \tau_{rz}(r, \theta) &= \frac{2P}{\alpha} \sum_{n=1}^{\infty} \frac{u_1 r^{m-1}}{u_1-u_2} \left\{ (-1)^n h_1^{-m} \left[ \left( \frac{r}{h_1} \right)^{u_1} - \left( \frac{a}{h_1} \right)^{u_2} \left( \frac{r}{a} \right)^{u_1} \right] \right. \\
 &\left. - h_2^{-m} \left[ \left( \frac{r}{h_2} \right)^{u_1} - \left( \frac{a}{h_2} \right)^{u_2} \left( \frac{r}{a} \right)^{u_1} \right] \right\} \cos\left(\frac{n\pi}{\alpha} \theta\right) \quad 0 \leq r < h_1
 \end{aligned} \quad (75a)$$

$$\tau_{rz}(r, \theta) = \frac{2P}{\alpha} \sum_{n=1}^{\infty} \frac{r^{m-1}}{u_1 - u_2} \left\{ (-1)^n h_1^{-m} \left[ u_2 \left( \frac{r}{h_1} \right)^{u_2} - u_1 \left( \frac{a}{h_1} \right)^{u_2} \left( \frac{r}{a} \right)^{u_1} \right] \right. \\ \left. - u_1 h_2^{-m} \left[ \left( \frac{r}{h_2} \right)^{u_1} - \left( \frac{a}{h_2} \right)^{u_2} \left( \frac{r}{a} \right)^{u_1} \right] \right\} \cos \left( \frac{n\pi}{\alpha} \theta \right) \quad h_1 < r < h_2 \quad (75b)$$

$$\tau_{rz}(r, \theta) = \frac{2P}{\alpha} \sum_{n=1}^{\infty} \frac{r^{m-1}}{u_1 - u_2} \left\{ (-1)^n h_1^{-m} \left[ u_2 \left( \frac{r}{h_1} \right)^{u_2} - u_1 \left( \frac{a}{h_1} \right)^{u_2} \left( \frac{r}{a} \right)^{u_1} \right] \right. \\ \left. - h_2^{-m} \left[ u_2 \left( \frac{r}{h_2} \right)^{u_2} - u_1 \left( \frac{a}{h_2} \right)^{u_2} \left( \frac{r}{a} \right)^{u_1} \right] \right\} \cos \left( \frac{n\pi}{\alpha} \theta \right) \quad h_2 < r \leq a \quad (75c)$$

$$\tau_{\theta z}(r, \theta) = \frac{2\pi P}{\alpha^2} \sum_{n=1}^{\infty} \frac{nr^{m-1}}{u_1 - u_2} \left\{ (-1)^n h_1^{-m} \left[ \left( \frac{a}{h_1} \right)^{u_2} \left( \frac{r}{a} \right)^{u_1} - \left( \frac{r}{h_1} \right)^{u_1} \right] \right. \\ \left. - h_2^{-m} \left[ \left( \frac{a}{h_2} \right)^{u_2} \left( \frac{r}{a} \right)^{u_1} - \left( \frac{r}{h_2} \right)^{u_1} \right] \right\} \sin \left( \frac{n\pi}{\alpha} \theta \right) \quad 0 \leq r \leq h_1 \quad (76a)$$

$$\tau_{\theta z}(r, \theta) = \frac{2\pi P}{\alpha^2} \sum_{n=1}^{\infty} \frac{nr^{m-1}}{u_1 - u_2} \left\{ (-1)^n h_1^{-m} \left[ \left( \frac{a}{h_1} \right)^{u_2} \left( \frac{r}{a} \right)^{u_1} - \left( \frac{r}{h_1} \right)^{u_2} \right] \right. \\ \left. - h_2^{-m} \left[ \left( \frac{a}{h_2} \right)^{u_2} \left( \frac{r}{a} \right)^{u_1} - \left( \frac{r}{h_2} \right)^{u_1} \right] \right\} \sin \left( \frac{n\pi}{\alpha} \theta \right) \quad h_1 \leq r \leq h_2 \quad (76b)$$

$$\tau_{\theta z}(r, \theta) = \frac{2\pi P}{\alpha^2} \sum_{n=1}^{\infty} \frac{nr^{m-1}}{u_1 - u_2} \left\{ (-1)^n h_1^{-m} \left[ \left( \frac{a}{h_1} \right)^{u_2} \left( \frac{r}{a} \right)^{u_1} - \left( \frac{r}{h_1} \right)^{u_2} \right] \right. \\ \left. - h_2^{-m} \left[ \left( \frac{a}{h_2} \right)^{u_2} \left( \frac{r}{a} \right)^{u_1} - \left( \frac{r}{h_2} \right)^{u_2} \right] \right\} \sin \left( \frac{n\pi}{\alpha} \theta \right) \quad h_2 \leq r \leq a \quad (76c)$$

It should be mentioned that in the particular case of an isotropic material we reach the same results as published by Kargarnovin et al. [11]. According to the reason mentioned in case IIa, the displacement field of a wedge with infinite radius should be identical to that of case Ic. The Eq. (60) may be obtained by taking the limit as  $a \rightarrow \infty$  in (74). The analyses respecting the behavior of stress and displacement fields in the vicinity of the act point of traction and the singularities of stress components in various cases of problem II are similar to those in the corresponding cases of problem I.

## 5 VERIFICATION

In order to verify the analytical solution, finite element simulation of the problem was performed using Abaqus 6.14-2 [30]. Problem Ia and IIb were selected for the purpose of verification. The values listed in Table 1 were used for material and loading definition.

USDFLD subroutine was employed to relate material property ( $\mu$ ) to the polar coordinates as defined in Eq. (2). For this purpose, a field variable ( $r$ ) was introduced as follows:

$$r = \sqrt{x^2 + y^2} \tag{77}$$

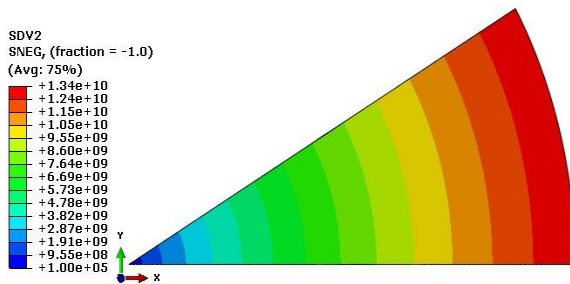
where  $x$  and  $y$  are components of Cartesian coordinates. Next, material property in terms of the defined field variable (Eq.(2)) were imported to the model as tabular values. 8-node quadratic quadrilateral elements with reduced integration (S8R) were employed for discretization of the domain. A mesh convergence study was performed. The dimensions of the element side were considered to be 0.0004, 0.0001 and 0.00005  $m$ . It was found that the elements with the size of 0.0001  $m$ , would provide converged stress. The whole model was discretized using 13751 elements and 41836 nodes. Distribution of  $\mu$  is illustrated in Fig. 3.

Fig. 4 shows the results of anti-plane deformation ( $w$ ) obtained from FE simulations and analytical solutions of problems Ia and IIb for the path passing through the line  $\theta = \pi/12$ . As can be seen from Fig. 4, the results of analytical solutions are in good agreement with the FE simulations for both problems.

**Table 1**

The value of parameters used in FE simulation.

Parameter	Value
$a$ (m)	0.1
$\alpha$ (rad)	$\pi/16$
$m$	0.5
$\mu_0$ (Pa)	$7.52 \times 10^{10}$
$P$ (N/m) - Problem Ia	10000000
$h$ (m) - Problem Ia	0.05
$k$ - Problem IIb	2.5



**Fig.3** Distribution of  $\mu$  in FG wedge.

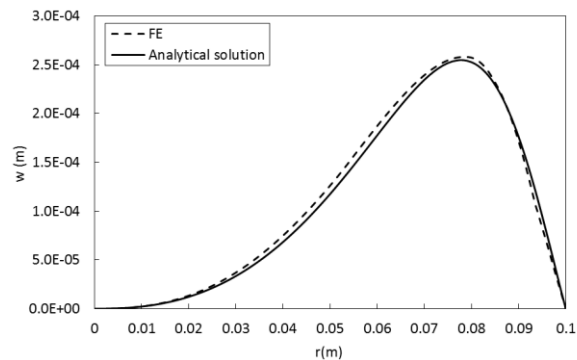
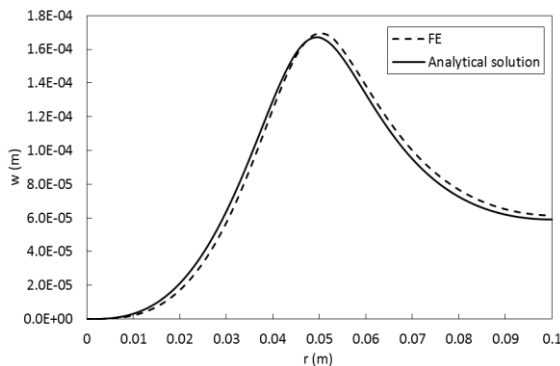


**Fig.4**

Results of anti-plane deformation obtained from FE simulations and analytical solutions for the path passing through the line  $\theta = \pi/12$  (a) Problem Ia (b) Problem IIb.

## 6 CONCLUSION

In the present paper, the stress analysis of a finite FGM wedge subjected to antiplane deformation was studied analytically. In order to solve the governing differential equation, the finite Fourier transforms and Green's function method was employed. The boundary condition on the arc segment is the zero displacement component in problem I and is traction free in problem II. For the radial edges, all possible boundary data were considered in each problem as three various cases: traction-displacement, displacement-displacement and traction-traction. For each of the cases, exact closed form solution was achieved for stress and displacement fields. Furthermore, in each case, the influences of material constant and apex angle on the order of stress singularity were discussed. For the particular case of a wedge with infinite radius, both problems produce the same results by applying  $a \rightarrow \infty$ . The results of the particular case of a wedge with isotropic materials may be extracted from the solutions of an FG wedge.

## REFERENCES

- [1] Tranter C.J., 1948, The use of the Mellin transform in finding the stress distribution in an infinite wedge, *The Quarterly Journal of Mechanics and Applied Mathematics* **1**: 125-130.
- [2] Williams M.L., 1952, Stress singularities resulting from various boundary conditions in angular corners of plates in extension, *Journal of Applied Mechanics* **19**: 526-528.
- [3] Bogy D.B., 1972, The plane solution for anisotropic elastic wedges under normal and shear loading, *Journal of Applied Mechanics* **39**: 1103-1109.
- [4] Kuo M.C., Bogy D.B., 1974, Plane solutions for the displacement and traction-displacement problems for anisotropic elastic wedges, *Journal of Applied Mechanics* **41**: 197-202.
- [5] Kuo M.C., Bogy D.B., 1974, Plane solutions for traction problems on orthotropic unsymmetrical wedges and symmetrically twinned wedges, *Journal of Applied Mechanics* **41**: 203-208.
- [6] Dempsey J.P., Sinclair G.B., 1979, On the stress singularities in the plane elasticity of the composite wedge, *Journal of Elasticity* **9**: 373-391.
- [7] Dempsey J.P., 1981, The wedge subjected to tractions: a paradox resolved, *Journal of Elasticity* **11**: 1-10.
- [8] Ting T.C.T., 1984, The wedge subjected to tractions: a paradox re-examined, *Journal of Elasticity* **14**: 235-247.
- [9] Ting T.C.T., 1985, Elastic wedge subjected to antiplane shear traction – a paradox explained, *The Quarterly Journal of Mechanics and Applied Mathematics* **38**: 245-255.
- [10] Ma C.C., Hour B.L., 1989, Analysis of dissimilar anisotropic wedges subjected to antiplane shear deformation, *International Journal of Solids and Structures* **25**: 1295-1309.
- [11] Kargarnovin M.H., Shahani A.R., Fariborz S.J., 1997, Analysis of an isotropic finite wedge under antiplane deformation, *International Journal of Solids and Structures* **34**: 113-128.
- [12] Shahani A.R., 1999, Analysis of an anisotropic finite wedge under antiplane deformation, *Journal of Elasticity* **56**: 17-32.
- [13] Shahani A.R., Adibnazari S., 2000, Analysis of perfectly bonded wedges and bonded wedges with an interfacial crack under antiplane shear loading, *International Journal of Solids and Structures* **37**: 2639-2650.
- [14] Shahani A.R., 2003, Mode III stress intensity factors for edge-cracked circular shafts, bonded wedges, bonded half planes and DCB's, *International Journal of Solids and Structures* **40**: 6567-6576.
- [15] Faal R.T., Fotuhi A.R., Fariborz S.J., Daghyani H.R., 2004, Antiplane stress analysis of an isotropic wedge with multiple cracks, *International Journal of Solids and Structures* **41**: 4535-4550.
- [16] Lin R.L., Ma C.C., 2004, Theoretical full-field analysis of dissimilar isotropic composite annular wedges under antiplane deformations, *International Journal of Solids and Structures* **41**: 6041-6080.
- [17] Shahani A.R., 2005, Some problems in the antiplane shear deformation of bi-material wedges, *International Journal of Solids and Structures* **42**: 3093-3113.
- [18] Shahani A.R., 2006, Mode III stress intensity factors in an interfacial crack in dissimilar bonded materials, *Archive of Applied Mechanics* **75**: 405-411.
- [19] Faal R.T., Fariborz S.J., Daghyani H.R., 2007, Stress analysis of a finite wedge weakened by cavities, *International Journal of Mechanical Sciences* **49**: 75-85.
- [20] Shahani A.R., 2007, On the antiplane shear deformation of finite wedges, *Applied Mathematical Modelling* **31**: 141-151.
- [21] Chen C.H., Wang C.L., Ke C.C., 2009, Analysis of composite finite wedges under anti-plane shear, *International Journal of Mechanical Sciences* **51**: 583-597.
- [22] Shahani A.R., Ghadiri M., 2009, Analysis of bonded finite wedges with an interfacial crack under antiplane shear loading, *The Proceedings of the Institution of Mechanical Engineers, Part C: Journal of Mechanical Engineering Science* **223**(10): 2213-2223.
- [23] Shahani A.R., Ghadiri M., 2010, Analysis of anisotropic sector with a radial crack under anti-plane shear loading, *International Journal of Solids and Structures* **47**: 1030-1039.

- [24] Ghadiri M., Shahani A.R., 2012, Mode III fracture analysis of an anisotropic finite wedge with an interfacial crack, *Mathematics and Mechanics of Solids* **7**: 1-14.
- [25] Ghadiri M., Shahani A.R., 2014, Analysis of bonded anisotropic wedges with interface crack under anti-plane shear loading, *Applied Mathematics and Mechanics* **35**(5): 637-654.
- [26] Eder M.A., Sarhadi A., 2020, A semi-analytical stress correction method for bi-material Mode-III V-notches, *Theoretical and Applied Fracture Mechanics* **106**: 102443.
- [27] Sneddon I.N., 1972, *The Use of Integral Transforms*, McGraw-Hill, New York.
- [28] Stakgold I., 2011, *Green's Functions and Boundary Value Problems*, Wiley, New York.
- [29] Duffy D.G., 2015, *Green's Functions with Application*, CRC Press, Boca Raton.
- [30] Dassault Systèmes, 2014, Abaqus Product Documentation: Abaqus Analysis User's Manual, Providence, RI, Version 6.14-2.